How widespread and important is N_2 fixation in the North Atlantic Ocean?

Sarah E. Reynolds,[1,2] Rhiannon L. Mather,[1] George A. Wolff,[1]
Richard G. Williams,[1] Angela Landolfi,[3,4] Richard Sanders,[3]
and E. Malcolm S. Woodward[5]

Received 8 November 2006; revised 25 June 2007; accepted 24 July 2007; published 21 November 2007.

[1] The spatial extent of N_2 fixation in the Atlantic Ocean is examined by determining the isotopic composition of N in suspended particulate organic nitrogen (δ^{15}N PON_{susp}). The samples were collected from zonal and meridional transects of the Atlantic Ocean during a 3-year period. There is a consistent depleted δ^{15}N PON_{susp} signal extending over the center of the northern subtropical gyre, which partly coincides with a region where the tracer N* increases westward following the gyre circulation. This nonconservative behavior of N* implies that N_2 fixation is responsible for the depleted δ^{15}N PON_{susp}. A mixing model suggests that N_2 fixation over parts of the northern gyre provides up to 74% of the N utilized by phytoplankton. However, since the PON_{susp} represents only a small fraction of the total N pool, N_2 fixation probably only plays a minor role in supplying new N to the euphotic zone in the surface waters of the northern subtropical gyre.

Citation: Reynolds, S. E., R. L. Mather, G. A. Wolff, R. G. Williams, A. Landolfi, R. Sanders, and E. M. S. Woodward (2007), How widespread and important is N_2 fixation in the North Atlantic Ocean?, *Global Biogeochem. Cycles*, *21*, GB4015, doi:10.1029/2006GB002886.

1. Introduction

[2] Large regions of the surface Atlantic Ocean are characterized by nutrient deficient waters, where the winds induce downwelling over subtropical gyres, to the north and south of the equator (Figure 1a). Over these oligotrophic gyres, carbon export rates are characteristically low; for example, only reaching 4.3 mol C m^{-3} a^{-1} at the BATS site in the western North Atlantic [*Michaels et al.*, 1994]. Nevertheless, their extensive area implies that ~50% of the global drawdown of oceanic organic carbon occurs over these downwelling regions [*Emerson et al.*, 1997]. The maintenance of carbon export in the subtropical gyres requires a supply of new nutrient to the surface ocean. However, for the North Atlantic subtropical gyre, there is a mismatch between the estimates of export of 0.42 to 0.56 mol N m^{-2} a^{-1} [*Jenkins and Goldman*, 1985] and supply of 0.27 mol N m^{-2} a^{-1} [*Jenkins and Goldman*, 1985; *McGillicuddy et al.*, 1998; *Williams and Follows*, 2003], respectively from and to the photic zone. Proposed mechanisms to supply additional N include upwelling of deep nitrate via local mesoscale eddies and fronts [*Levy et al.*, 2001; *McGillicuddy et al.*, 1998], lateral advection of dissolved organic nitrogen [*Roussenov et al.*, 2006] and N_2 fixation [*Gruber and Sarmiento*, 1997; *Mahaffey et al.*, 2005] (Figure 2a).

[3] Direct fixation of molecular N by marine diazotrophs, particularly the extent to which it fuels primary production in oligotrophic oceans, has been discussed extensively in the literature [e.g., *Karl et al.*, 2002; *Mahaffey et al.*, 2005; *Capone et al.*, 2005]. *Trichodesmium* sp. have long been recognized as important N_2 fixing cyanobacteria [*Capone et al.*, 1997; *Carpenter et al.*, 1997; *Tyrrell et al.*, 2003]; more recently unicellular diazotrophs have also been found to play a role in the supply of N to surface waters [*Montoya et al.*, 2004].

[4] The relative abundances of the naturally occurring stable isotopes of N, ^{15}N and ^{14}N (δ^{15}N), have the potential to identify sources of N utilized by phytoplankton and subsequent transformations through the water column (Figure 2b). A unique data set is presented here of the isotopic composition of suspended particulate organic nitrogen (δ^{15}N PON_{susp}) collected over 3 years (2003 to 2006) in the Atlantic Ocean from four meridional transects (as part of the Atlantic Meridional Transect program [see *Robinson et al.*, 2006]) and two zonal transects across the North Atlantic basin (Figure 1b). This data set provides a large scale context to understand the different nitrogen supply mechanisms to the primary producers in the surface

[1]Department of Earth and Ocean Sciences, University of Liverpool, Liverpool, UK.
[2]Now at Department of Ocean, Earth and Atmospheric Sciences, Old Dominion University, Norfolk, Virginia, USA.
[3]National Oceanography Centre, University of Southampton Waterfront Campus, Southampton, UK.
[4]Now at Biogeochemical Modeling, Leibniz Institute of Marine Sciences, Kiel, Germany.
[5]Plymouth Marine Laboratory, Plymouth, UK.

0886-6236/07/2006GB002886

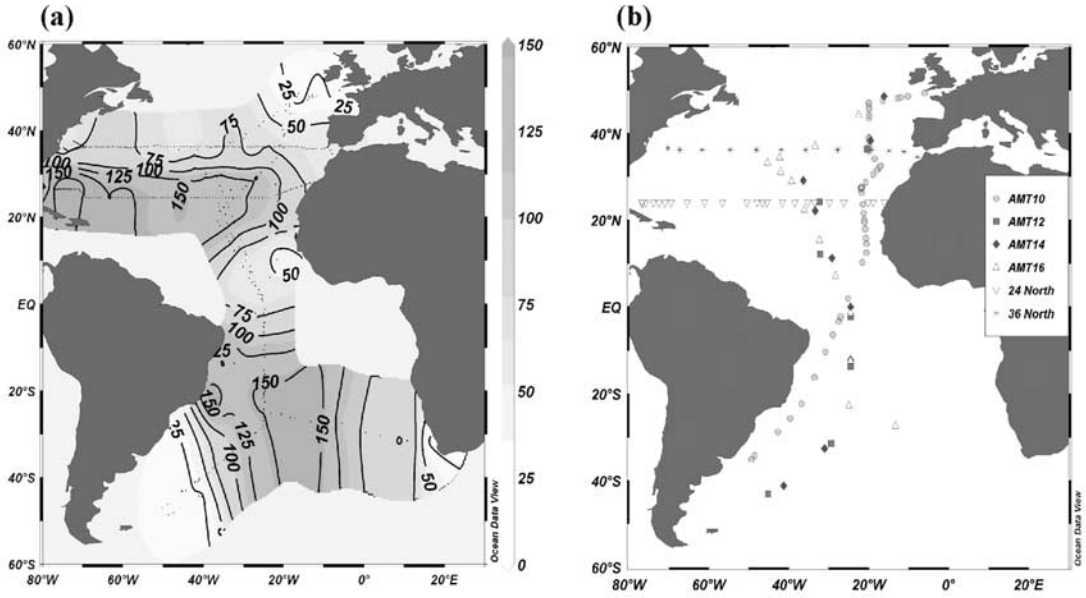

Figure 1. (a) Composite map of the depth of the nitricline (1 μM NO_3^-) over the Atlantic Basin. Deeper nitricline observed in the northern and southern basin is referred to as oligotrophic gyres, whereas a much shallower nitricline appears at the equator. (b) Meridional and zonal cruise tracks in the Atlantic Ocean incorporated in this study.

ocean and complements the Bermuda Atlantic Time series Study (BATS) nitrogen isotopic data [*Altabet*, 1988; *Knapp et al.*, 2005].

[5] The aims of this study were: (1) to determine the δ^{15}N PON_{susp} in surface waters (upper 150 m) along transects of the North Atlantic and to identify its large-scale spatial, seasonal and inter-annual variability and (2) to interpret the δ^{15}N PON_{susp} signals in terms of the sources of N utilized by phytoplankton, particularly focusing on N_2 fixation and to identify its relative importance.

2. Approach

2.1. Stable Nitrogen Isotopes as a Tool in Identifying N Pathways

[6] The study of δ^{15}N in water has revealed how the phototrophic assimilation of nitrogen operates and its dynamics in aquatic ecosystems [*Fogel and Cifuentes*, 1993]. While the two stable isotopes, ^{14}N and ^{15}N (99.634% and 0.366% by atoms respectively) behave chemically in a similar way to one another [*Owens*, 1987], during uptake of inorganic N by marine microorganisms, ^{14}N is preferentially consumed relative to the heavier ^{15}N isotope leading to biological fractionation in favor of the lighter isotope in the organisms cell [*Montoya and McCarthy*, 1995]. However, in environments such as the oligotrophic regions of the Atlantic Ocean where nitrogen is limiting, nitrogen is completely sequestered by the autotroph, there is no fractionation and the isotopic composition of the source-N is reflected within the organism [*Altabet and McCarthy*, 1985] (Figure 2b).

[7] The key sources of N are now briefly discussed in terms of their isotopic signal. Atmospheric N_2 made available via nitrogen fixation gives rise to an isotopically depleted signal of −2‰ to 0‰ for the δ^{15}N PON_{susp}, since no fractionation occurs during uptake [*Minagawa and Wada*, 1986]. NO_3^- found in rain has an isotopic signal of −2.1‰ to −5.9‰ [*Hastings et al.*, 2003] which could also result in depleted δ^{15}N PON_{susp}. In contrast, deep nitrate is isotopically enriched with values in the Atlantic Ocean ranging between 4.5‰ and 6‰ [*Knapp et al.*, 2005; *Liu and Kaplan*, 1989; *Sigman et al.*, 1997]. The enriched signal of nitrate reflects the remineralization of PON, principally from the suspended particulate organic nitrogen (PON_{susp}) rather than the sinking pool (PON_{sink}). The more abundant PON_{susp} pool becomes isotopically enriched with depth through progressive decomposition and removal of dissolved N species depleted in ^{15}N [*Altabet*, 1988]. The δ^{15}N PON_{sink} is also initially enriched with depth [*Altabet*, 1996], although δ^{15}N PON_{sink} then becomes isotopically depleted deeper in the ocean interior, either due to a loss of an enriched N fraction or by sorption of ^{14}N rich compounds [*Altabet et al.*, 1991; *Nakatsuka et al.*, 1997; *Voss et al.*, 1996]. The isotopic signature of dissolved organic nitrogen (DON) is also important, since aside from molecular N_2, it is the largest available nitrogen pool in the surface waters of the oligotrophic gyres (Figure 2a) [*Berman and Bronk*, 2003; *Jackson and Williams*, 1985; *Mahaffey et al.*, 2004]. At BATS, δ^{15}N values for DON were consistently found to be in the range of 3.5‰ to 4.5‰ in the upper 100 m over 12 months. However, the stability in both concentrations and the N isotopic composition of DON suggests that this DON pool is mainly recalcitrant and not assimilated by phytoplankton [*Knapp et al.*, 2005].

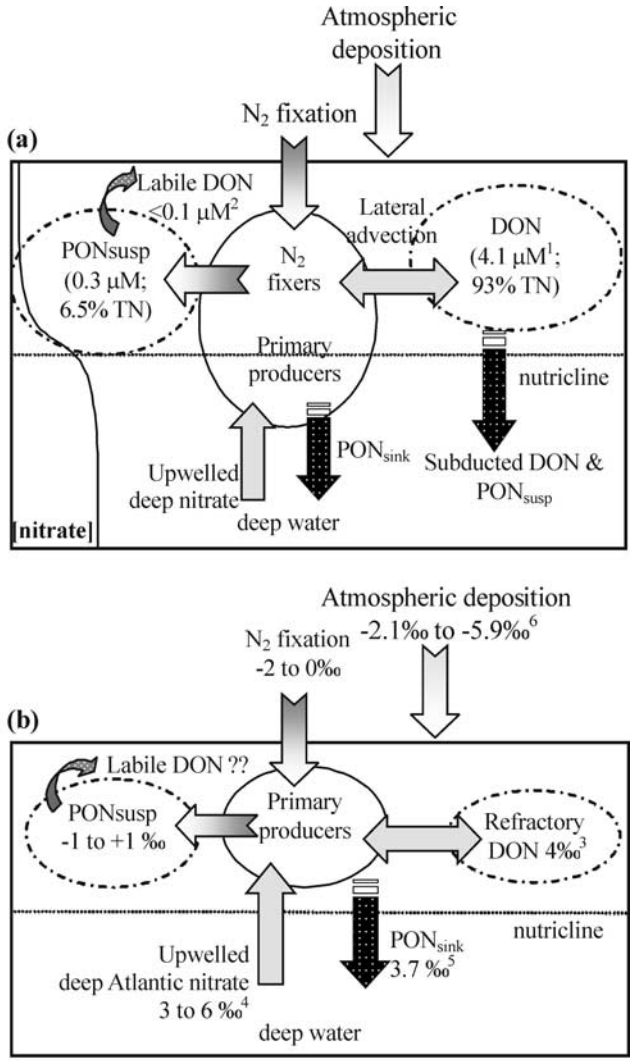

Figure 2. (a) Pathways of N through the oligotrophic ocean. Proposed mechanisms fuelling primary production include upwelling of deep NO_3^-, advection of DON, and N_2 fixation. Typical DON values (averaged above 1 μM nitricline) for the North Atlantic subtropical gyre (NASG) are given. Mean value of PON_{susp} (averaged above 1 μM nitricline) over the NASG are given. (b) Pathways of N with corresponding $\delta^{15}N$ within the oligotrophic Atlantic Ocean. The $\delta^{15}PON_{sink}$ is taken from 100-m sediment trap. Superscripts denote the following: 1, S. Torres, personal communication, 2006; 2, *Mahaffey et al.* [2004]; 3, *Knapp et al.* [2005]; 4, *Knapp et al.* [2005] and *Liu and Kaplan* [1989]; 5, *Altabet* [1988]; and 6, *Hastings et al.* [2003].

2.2. Methodology

2.2.1. Sampling Protocol

[8] Suspended particulate organic nitrogen samples on AMT 12, 14, 16, 17 and 36°N cruises were collected using Stand Alone Pumps (SAPs; Challenger Oceanic; Figure 1b and Table 1). Two GF/F filters (293 mm diameter; Whatman; pre-combusted at 400°C, >4 hours) were placed on the filter bed with the top filter being used for the analysis. The SAPs were deployed to depths of 50, 100 and 150 m and pumped ~1000 L seawater in 90 min. The filters were wrapped in precombusted (400°C > 4 hours) aluminum foil and frozen (−20°C) until further analysis in the laboratory. Prior to analysis, filters were lyophilized (−60°C; 10^{-2} Torr, 24 hours).

[9] PON samples collected on the 24°N cruise (Figure 1b and Table 1) were from Niskin bottles fired in surface waters (10 to 25 m). Seawater (8 L) was filtered through GF/F filters (47 mm diameter; Whatman; precombusted at 550°C, 4 hours) using an acid (HCl) washed glass filtration unit (1 L). Filters were then folded and placed into pre-combusted aluminum foil (550°C; 4 hours) and then frozen (−20°C) until further analysis in the laboratory. Prior to analysis, filters were dried (60°C; 24 hours) and stored in a dessicator [*Landolfi*, 2005].

2.2.2. Determination of PON, POC, and Chlorophyll *a*

[10] Concentrations of particulate organic carbon (POC) and particulate nitrogen (PN) were determined from freeze-dried SAPS filters [*Kiriakoulakis et al.*, 2004]. Analyses of the filters were carried out in duplicate (analytical error <10%; CEInstruments NC 2500 CHN analyzer), on aliquots of known area (~130 mm^2), using the acid HCl vapor method of *Yamamuro and Kayanne* [1995]. Chlorophyll *a* concentrations were determined from Niskin water bottle samples and the underway non-toxic water supply using a fluorometric assay of the acetone extract of particulate material collected on a GF/F filter [*Welschmeyer*, 1994]. Chlorophyll *a* concentrations were also obtained from an in situ fluorometer fitted on the CTD rosette sampler frame, data being calibrated against the field samples.

2.2.3. Determination of $\delta^{15}N$ PON_{susp}

[11] Isotopic analyses of the PON_{susp} were carried out directly on filter aliquots (314 mm^2) without decarbonation. The AMT12, 14, 16, 17 and 36°N samples were analyzed using a Thermo Finnigan Delta-Plus Advantage isotope ratio mass spectrometer (IRMS), coupled to a Costech Instruments ECS 4010 elemental combustion system ("EA") via a Thermo Finnigan Conflo III open-split interface. The EA was equipped with a Costech Zero Blank autosampler, utilizing a 32-position, large-capacity sample wheel. For 24°N samples a Eurovector 3028-Ht elemental analyzer connected to a GV Isoprime mass spectrometer was employed. Sample $\delta^{15}N$ ratios were measured relative to atmospheric nitrogen, where

$$\delta^{15}N = \left[\frac{\left(^{14}N/^{15}N\right)_{sample}}{\left(^{14}N/^{15}N\right)_{standard}} - 1 \right] \times 100\%, \quad (1)$$

with the samples calibrated against a variety of primary standards, and normalized for weight-to-δ bias and calibration offset using a secondary isotope ratio standard (acetanilide).The samples for the AMT and 36°N cruises were analyzed in duplicate and the precision is based upon taking the variation of the mean of the two measurements made and was found to be ±0.5‰. The accuracy of the analysis was determined as ±0.4‰ by combining errors associated with measuring both the primary standards and the acetanilide standard.

Table 1. Cruise Details and Methods of PON_{susp} Collection[a]

Cruise	Boreal Season	Dates, dd/mm/yy	From	To	Method
AMT10	Spring	12/04/00 to 07/05/00	Montevideo, Uruguay	Grimsby, UK	CTDs and underway
AMT12	Spring	12/05/03 to 14/6/03	Port Stanley, Falklands	Grimsby, UK	SAPs
AMT14	Spring	26/04/04 to 02/06/04	Port Stanley, Falklands	Grimsby, UK	SAPs
AMT16	Spring	19/05/05 to 29/06/05	Cape Town, SA	Falmouth, UK	SAPs
AMT17	Autumn	15/10/05 to 28/11/05	Clyde, UK	Port Elizabeth, SA	SAPs
24° North	Spring	04/04/04 to 10/05/04	Freeport, Grand Bahama	Santa Cruz de Tenerife	CTDs
36° North	Spring	01/05/05 to 15/06/05	St. Georges Bermuda	Lisbon, Portugal	SAPs

[a]See also Figure 1b. AMT10 data have been previously reported [*Mahaffey et al.*, 2004, 2003].

2.2.4. Determination of Inorganic Nitrate and Phosphate

[12] Inorganic nitrate and phosphate concentrations in seawater samples collected on AMT12, 14, 16 and 17 were analyzed using a Technicon segmented flow colorimetric autoanalyzer [*Woodward and Rees*, 2001]. Analytical precision was ±2–4% with reproducibility errors in the same range. For 24°N and 36°N cruises, inorganic nitrate and phosphate were measured using a Skalar San^{Plus} continuous flow autoanalyzer [*Sanders and Jickells*, 2000].

2.3. Validity of Data: Trophic Tests

[13] PON_{susp} is derived from phytoplankton, but may also be modified by organisms from higher trophic levels by grazing and the microbial loop. When N is assimilated by zooplankton, there is an enrichment of ~3‰ [*Minagawa and Wada*, 1986], which is significant when using isotopic data to infer N sources to the phytoplankton. In order to determine if higher trophic particulate material has affected the measured $\delta^{15}N$ in the present study, the relationships between POC and PON:$\delta^{15}N$ PON_{susp} with chlorophyll *a* were examined. Organisms of higher trophic levels feeding on suspended particles significantly alter both POC and PON_{susp}, leading to enhanced values of POC/Chlorophyll *a* and PON/Chlorophyll *a* [*Waser et al.*, 2000]. *If* the PON_{susp} material measured is principally derived from heterotrophs rather than autotrophs, a positive relationship would be expected between these ratios and $\delta^{15}N$ PON_{susp}. At a confidence level of 95% ($P < 0.05$; T-test), no statistically significant positive or negative relationship was found in the individual or collective cruise data sets, which implies that

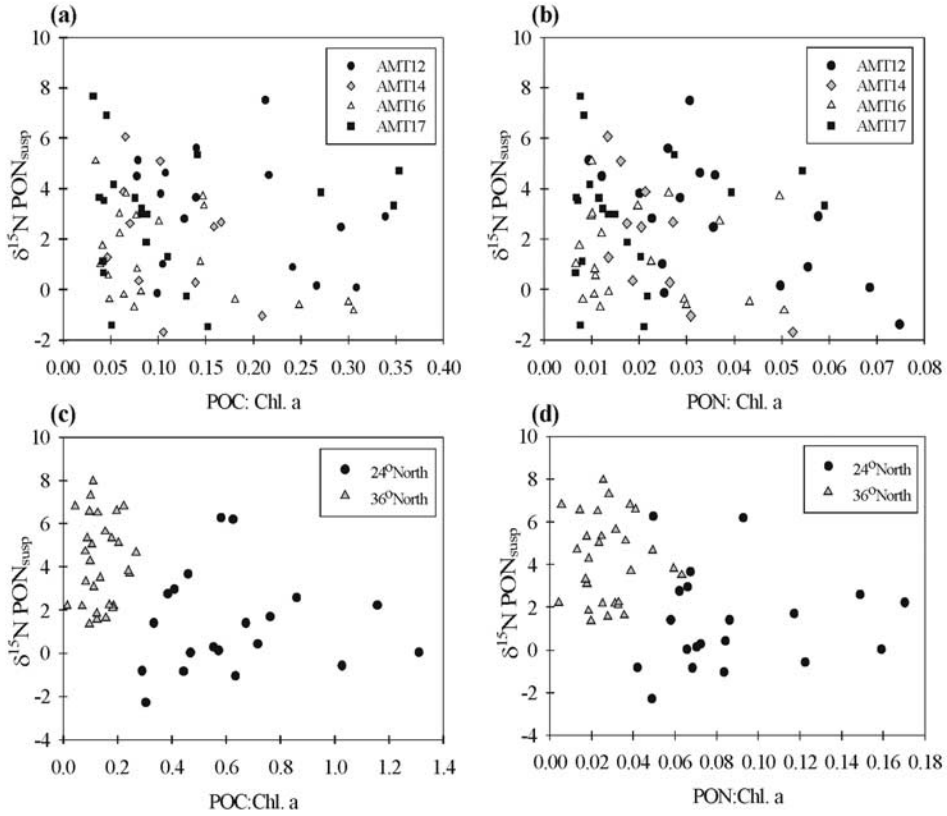

Figure 3. Trophic tests to determine if $\delta^{15}N$ PON_{susp} is strongly influenced by higher trophic organisms [*Waser et al.*, 2000]. The lack of any significant relationship demonstrates that the PON_{susp} predominantly comprises of primary particulate material.

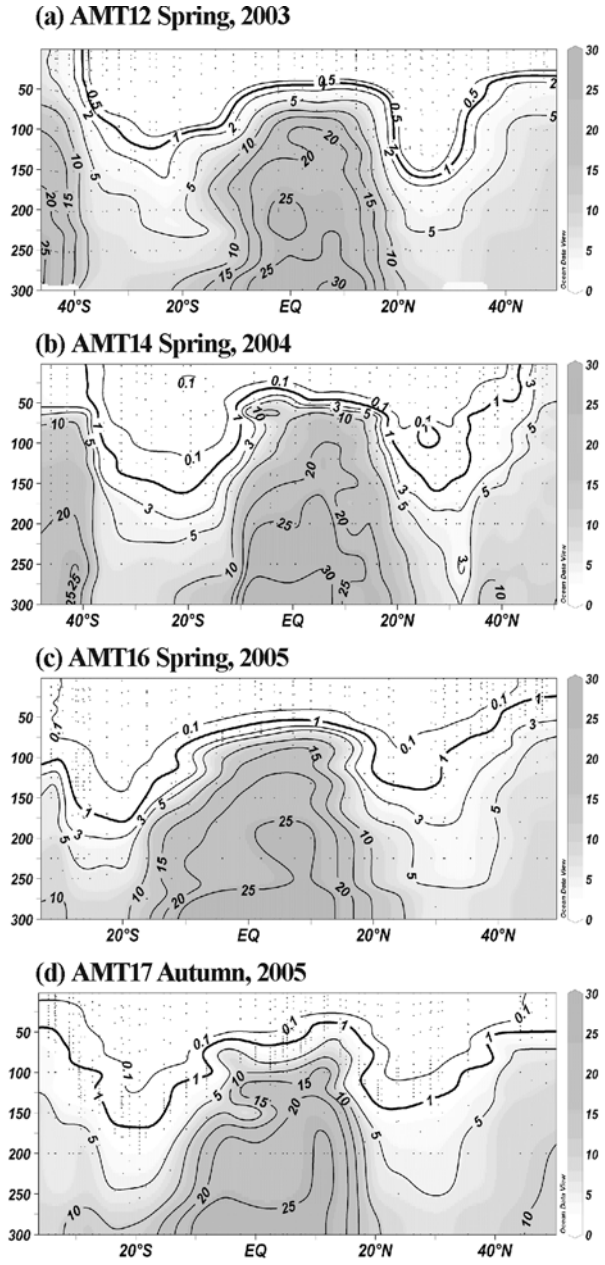

Figure 4. Meridional nitrate (μM) sections labeled with Northern Hemisphere season, with the nitricline defined at 1 μM. The nitricline varies in a consistent manner both annually and seasonally. Strong upwelling is observed at the equator while there is a characteristic deep nitricline witnessed to the north and south of the equator, which characterizes oligotrophic gyres.

the measured δ^{15}N PON_{susp} is representative of autotrophic PON (Figure 3).

3. Nitrate and Isotopic N Distributions

3.1. Nitricline Structure of the Atlantic Ocean

[14] The AMT cruise transects pass through distinct biogeochemical regimes of the Atlantic Ocean as revealed by the variations in the nitrate concentrations of the upper 300 m of the water column (Figure 4). The nitricline varies meridionally, reflecting the background gyre structure and pattern of convection (Figures 4a–4d). The nitricline is deepest over the central parts of the subtropical gyres where there is downwelling and subduction (30°N and 25°S), and is shallowest in the tropics where upwelling occurs (10°S to 15°N). The nitricline also shallows poleward from the subtropical gyres, typically outcropping at 40°S in the south Atlantic and north of 45°N in the northern subpolar gyre.

[15] There is a general westward deepening of nutrient surfaces below the 1 μM isopleths within the northern subtropical gyre, reflecting the deepening of the thermocline through Ekman pumping (Figures 5a and 5b). The increasing depth of the nitricline from the eastern to western basin boundary is more pronounced along the 24°N than the 36°N transect. In addition, at the eastern boundary of the 24°N transect (Figure 5a) there are higher concentrations of nitrate, which decrease considerably westward into the centre of the oligotrophic gyre. A similar pattern is apparent along the 36°N transect (Figure 5b), although concentrations of nitrate are lower at the eastern edge of the gyre and are elevated in the western boundary current.

3.2. Spatial Variability of the δ^{15}N PON_{susp} in the Atlantic Ocean

[16] The δ^{15}N PON_{susp} has been measured in the Atlantic Ocean between 45°S and 50°N (AMT12, 14, 16 and 17) and along 24°N and 36°N. In order to consider the general variations in the δ^{15}N PON_{susp}, the data have been averaged

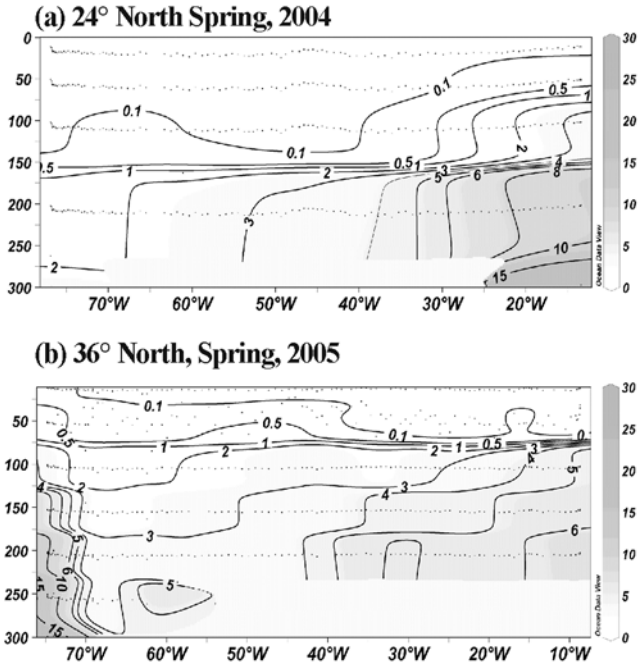

Figure 5. Zonal nitrate (μM) sections labeled with Northern Hemisphere season. Oligotrophic waters are observed in the western North Atlantic basin with eastward shallowing of the nitricline.

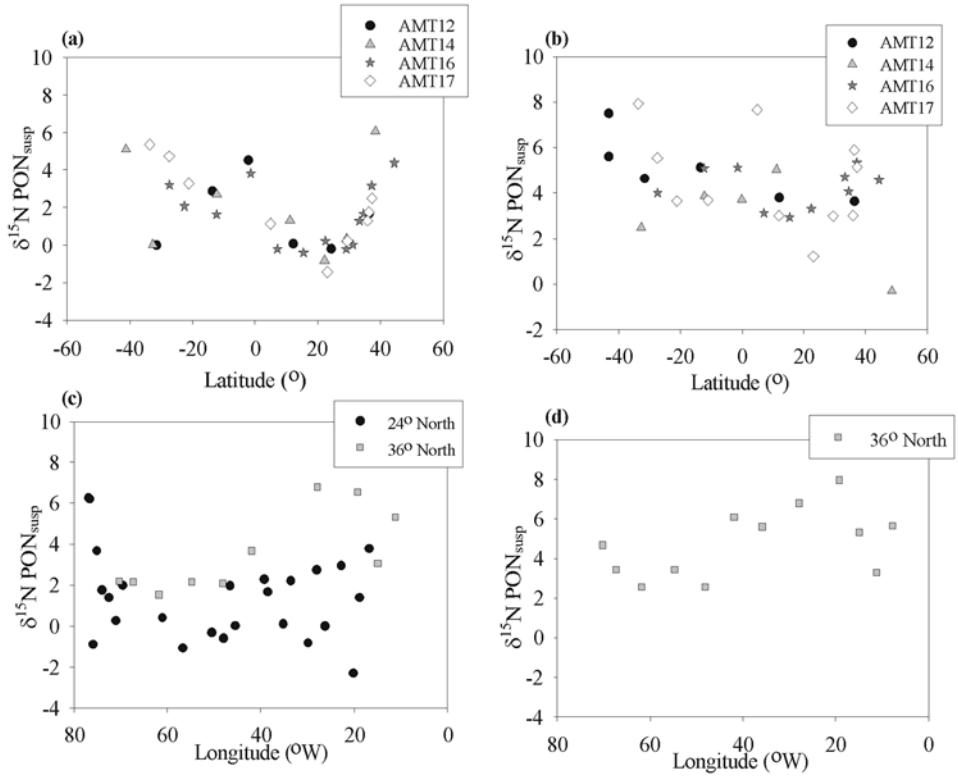

Figure 6. Meridional variations in δ^{15}N PON_{susp} (a) above the nitricline (values averaged) and (b) below the nitricline. Zonal variations in δ^{15}N PON_{susp} (c) above the nitricline and (d) below the nitricline.

separately above and below the nitricline (previously defined at 1 μM).

3.2.1. Spatial Variability Above the Nitricline

[17] For the meridional sections (Figure 6a), there is a consistent depleted signal (−1 to 0‰) in the northern basin between 7°N and 32°N for both the Northern Hemisphere spring (AMT12, 14 and 16) and autumn (AMT17). In the southern gyre, enriched values of 5‰ are found at 40°S and generally become depleted to reach a minimum of ∼2‰ at 12°S. A small depleted region (∼0‰) is found at 32°S. These data represent the Southern Hemisphere autumn (AMT12 and 14), whereas the more enriched values at a similar location derive from the Southern Hemisphere spring. Therefore, while δ^{15}N PON_{susp} in the northern gyre is consistently depleted, the southern gyre appears to show some seasonality. The δ^{15}N PON_{susp} is enriched at the equator (4‰) and along the northern flanks of the northern gyre (4–6‰).

[18] The zonal section along 24°N also shows a depleted signal of −1‰ from 56°W to 45°W (Figure 6c). There are enriched values (6‰) on the western boundary of the gyre at 80°W. However, on the eastern side of the gyre at 30°W, δ^{15}N PON_{susp} is depleted, with values of 0‰ to 1‰. Along 36°N, δ^{15}N PON_{susp} values are more enriched (Figure 6c) than along 24°N and δ^{15}N PON_{susp} increases eastward from 2.2‰ at 60°W to a maximum of 6.8‰ at 28°W.

3.2.2. Spatial Variability Below the Nitricline

[19] Meridional sections of the δ^{15}N PON_{susp} reveal a more enriched signal, as expected, below the nitricline (Figure 6b) compared with above the nitricline. The southern gyre (3.7–5.5‰) is slightly more enriched than the northern gyre (3–4‰), with even greater enrichment (6–8‰) being observed at the equator, at the southern flanks of the southern gyre and at the northern flanks of the northern gyre. A zonal section of the δ^{15}N PON_{susp} again reveals samples being slightly more enriched below the nitricline (Figure 6d) (only shown for 36°N data) compared with above the nitricline, and there is the same general pattern of enrichment from west to east.

4. How Are the δ^{15}N PON_{susp} Signals Controlled?

4.1. Enriched Signals

[20] At the equator, the enriched δ^{15}N PON_{susp} signal coincides with the nitricline (>1 μM) shoaling to depths as shallow as 40 m and is attributed to the wind-induced upwelling of nitrate rich waters. Deep Atlantic nitrate has a δ^{15}N range of 4.5‰ to 6‰ at depths greater than 500 m [*Knapp et al.*, 2005; *Liu and Kaplan*, 1989]. On the northern flank of the northern gyre, isotopic enrichment might result from deep NO_3^- supplied by convection at the end of the winter. On the southern flank of the southern gyre, the enriched δ^{15}N PON_{susp} implies a source of deep NO_3^-, probably supplied as part of the northern transport of intermediate waters from the Southern Ocean.

[21] The enrichment in isotopic values with depth in the oligotrophic gyres shows a strong relationship with the

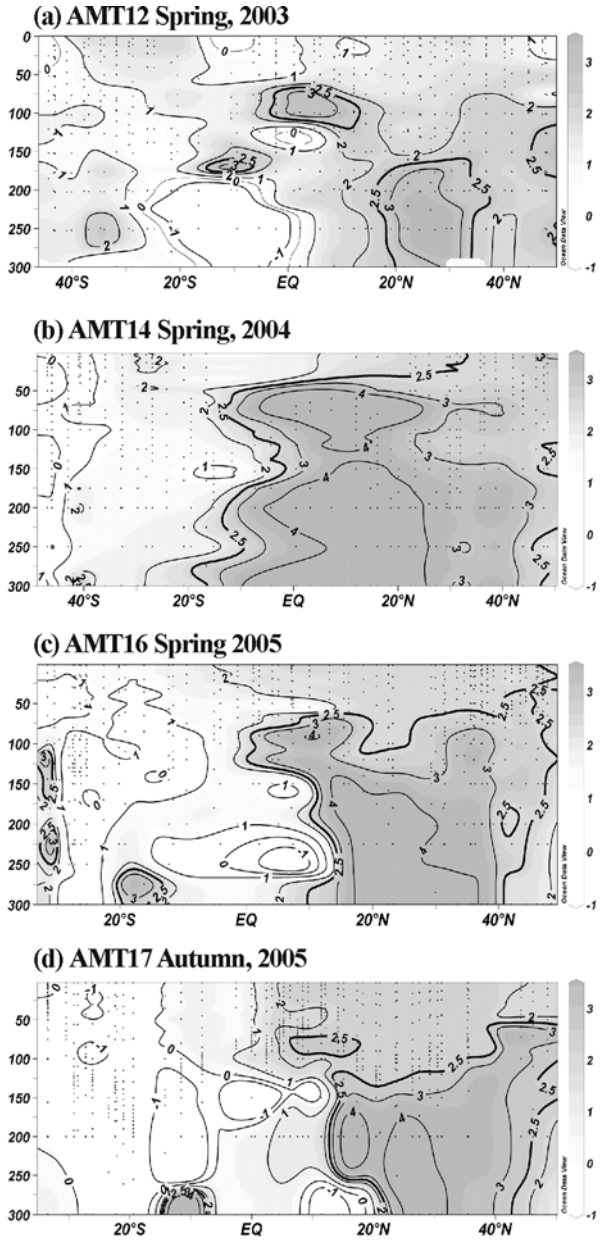

Figure 7. Plotted latitudinal sections of N* in the upper 300 m of the Atlantic Ocean labeled with the boreal seasons (a) AMT12, (b) AMT14, (c) AMT16, and (d) AMT17. There is a consistently elevated N* below the euphotic zone in the northern gyre.

nitricline. Phytoplankton lying at or below the nitricline may utilize deep nitrate leading to enriched δ^{15}N PON_{susp} and this may explain the isotopic gradient in the photic zone. Alternatively, the enrichment of δ^{15}N PON_{susp} with depth may simply reflect its greater degree of degradation [*Altabet*, 1988].

[22] The enrichment in δ^{15}N PON_{susp} from the Southern Hemisphere autumn to the Southern Hemisphere spring in the south Atlantic can be attributed to deepening of the mixed layer. During the winter months the mixed layer thickens and entrainment of deeper waters leads to a supply of nutrients to surface phytoplankton [*Polovina et al.*, 1995]. The more enriched δ^{15}N PON_{susp} during the Southern Hemisphere spring (AMT17) in the southern gyre might be the result of uptake of the deep enriched nitrate that was entrained into the euphotic zone during the previous winter.

4.2. Depleted Signals

[23] The low values of δ^{15}N PON_{susp} within the northern and southern oligotrophic gyres of the Atlantic Ocean might reflect three distinct N sources.

[24] 1. One possible source is uptake of remineralized compounds excreted by zooplankton, principally NH_4^+ [*Biggs*, 1977; *Corner and Davies*, 1971], which are depleted in ^{15}N. In oligotrophic regions, where phytoplankton take up and assimilate all nitrogen excreted by zooplankton, there is little or no overall isotopic fractionation [*Checkley and Miller*, 1989] and thus, δ^{15}N PON_{susp} is depleted.

[25] 2. Direct fixation of dissolved N_2 by marine diazotrophs gives rise to depleted δ^{15}N of PON [*Carpenter et al.*, 1997; *Mahaffey et al.*, 2003; *Minagawa and Wada*, 1986].

[26] 3. Uptake of isotopically light N supplied to the surface ocean by atmospheric deposition could give rise to depleted δ^{15}N PON_{susp} [*Hastings et al.*, 2003].

[27] Modeled atmospheric fluxes of N to the surface North Atlantic Ocean are only in the range of 0.003–0.007 mol N m^{-2} a^{-1} [*Dentener et al.*, 2006; *Galloway et al.*, 2004; *Prospero et al.*, 1996]. In situ aerosol measurements along the AMT transect showed a dry N deposition flux of ~0.01 mol N m^{-2} a^{-1} [*Baker et al.*, 2003] in the same region where there is the depleted signal of δ^{15}N PON_{susp} in the northern subtropical gyre. These estimates of atmospheric deposition appear to be relatively unimportant in sustaining export production, since they are much smaller than the export flux of 0.42 and 0.56 mol N m^{-2} a^{-1} determined for the western subtropical North Atlantic [*Jenkins and Goldman*, 1985].

[28] Hence N_2 fixation or the uptake of regenerated N are the most likely processes responsible for the depleted δ^{15}N PON_{susp}. To distinguish between the two processes, the relative size of the NO_3^- and PO_4^{3-} pools can be considered. Redfield stoichiometry [*Redfield*, 1958] is perturbed by N_2 fixation in favor of NO_3^- relative to PO_4^{3-}. A quasiconservative tracer, N*, which utilizes a linear combination of NO_3^- and PO_4^{3-} (2) has been used to define the distribution of N_2 fixation and denitrification at the basin scale [*Gruber and Sarmiento*, 1997],

$$N^* = \left(N - 16P + 2.90\ \mu\text{mol kg}^{-1}\right)0.87. \quad (2)$$

[29] *Gruber and Sarmiento* [1997] suggest that high values of N* are due to the remineralization of N-rich organic matter from diazotrophic organisms (see section 4.3.2 for further analysis). Meridional sections of the upper 300 m of the Atlantic over 3 years reveal that high N* values consistently lie below the photic zone in the northern gyre (Figure 7). These signals are in accord with the climatological analysis of *Gruber and Sarmiento* [1997].

[30] The localized region of depleted δ^{15}N PON_{susp} at 32°S found in the austral autumn might be due to a localized patch of N_2 fixation or through uptake of remineralized N,

since N* values lie between 1 and −1 over the entire southern basin (Figure 7). However, the data set for the South Atlantic is rather limited and it is difficult to provide a reliable explanation for the depleted δ^{15}N PON_{susp} signal there.

4.3. Synthesis of the Atlantic Ocean

4.3.1. Spatial Extent of the Depleted Isotopic N Signal

[31] A synthesis of δ^{15}N PON_{susp} data for samples collected above the nitricline has been made by collating data from the present study (excluding AMT17 which sailed in the Northern Hemisphere autumn) and from AMT10 surveyed in the Northern Hemisphere spring 2000 [*Mahaffey et al.*, 2004, 2003] (Figure 8a). In the northern gyre between 25°W and 55°W, there is an extensive region of depleted δ^{15}N PON_{susp}, while elevated values occur in the more temperate waters of the Northeast Atlantic and off the west coast of Africa. In the South Atlantic, there are low values of δ^{15}N PON_{susp} in the center of the subtropical gyre, with more enriched values off the east coast of South America and at the equator.

[32] The robustness of these signals is assessed by calculating the standard deviation (σ) and the standard error ($\sigma/\sqrt{n}$) based upon the number of independent data points (n) (Figures 8c and 8d). Within the northern gyre, the zone of depleted δ^{15}N reveals little variability and low standard errors are implied from the independent data points. Thus, the extensive region of depleted δ^{15}N PON_{susp} appears to be a robust signal. However, on the eastern side of the north Atlantic basin, there is a large standard deviation and standard error, reflecting how conditions are more variable there with upwelling off the west coast of Africa and convection in the north east Atlantic. The variability of the signals in the South Atlantic is small where there is data, but the data coverage is too limited to infer any robust signals.

4.3.2. Spatial Extent of Elevated N*

[33] The depleted δ^{15}N PON_{susp} signal in the northern subtropical gyre coincides with N* having a local maximum between 10°N and 30°N in the centre of the gyre (Figures 9a and 9b). N_2 fixation is only reliably implied from N* when this tracer increases following the flow [*Deutsch et al.*, 2001]; that is, N_2 fixation leads to enhanced N:P ratios in the underlying thermocline following a moving water mass. Thus elevated N* over the North Atlantic only provides a crude bulk measure of N_2 fixation occurring in the basin, instead, it is the gradient in N* created by horizontal transport which is a more accurate indicator of the source region. Comparing our N* signals (Figure 9b) and the latest drifter data (Figure 9c) [*Lumpkin and Pazos*, 2006] suggests that the local maximum in N* occurs where there is westward flow on the southern flank of the subtropical gyre. Thus, in our view, the most likely region of N_2 fixation in the North Atlantic is between 30°W–50°W and 15°N–30°N, where there is both depleted δ^{15}N PON_{susp} and a westward increase in N* following the gyre circulation.

[34] This region of potential N_2 fixation is subject to enhanced dust inputs from the Saharan Desert, which provide the limiting nutrients (P and Fe) for marine diazotrophs [*Mills et al.*, 2004] and creates an ideal niche for N_2 fixation to occur. In support of this view, *Mahaffey et al.* [2003] reported a natural fertilization event in the Northeastern Atlantic with coincident signals of depleted δ^{15}N PON_{susp}, phytopigments indicative of cyanobacteria and prochlorophytes, and elevated N:P ratios in the thermocline.

4.3.3. N_2 Fixation: Local or Far-Field Signatures?

[35] The region of depleted δ^{15}N PON_{susp} appears to be more confined than the N* signal, which extends over much of the North Atlantic. This mismatch poses the question of whether these independent signals reflect local or far field control? It has been previously suggested that the N* signal could be advected around the northern basin with the gyre circulation [*Hansell et al.*, 2004]. While at the surface, NO_3^- and PO_4^{3-} have very short residence times due to their rapid uptake by photoautotrophs, below the euphotic zone these nutrients are not utilized rapidly. Therefore, the NO_3^- and PO_4^{3-} can be advected within the thermocline without much modification and, thus, distribute the N* signal around the northern gyre. In turn, the isotopic signal might partially reflect the effect of advection. However, the lifetime of PON_{susp} is only 30 to 60 days in the euphotic zone [*Charette et al.*, 1999] suggesting that PON_{susp} might be advected 150 to 300 km, assuming a typical surface velocity of 5 cm s^{-1} in the gyre interior. Therefore the different extent of the N* and depleted N isotopic signals reflect their different lifetimes.

5. Significance of N_2 Fixation Within the North Atlantic

5.1. Role of N_2 Fixation in Providing New N to PON_{susp}

[36] There has been some controversy surrounding the importance of N_2 fixation as a source of new N to the oligotrophic regions of the North Atlantic. At BATS in the Sargasso Sea, the percentage contribution of new N from N_2 fixation [*Knapp et al.*, 2005] determined both from direct in situ rate measurements and geochemical estimates varies from 2% [*Orcutt et al.*, 2001] to 8% [*Gruber and Sarmiento*, 1997]. A simple two-end-member mixing model (3) is applied to the present North Atlantic data set in order to estimate the percentage contribution of new N supplied via N_2 fixation through the PON_{susp} pool (Table 2).

[37] The domain is separated into a region on the western side of the subtropical gyre (65°W–80°W, 20°N–40°N), the center of the oligotrophic gyre (30°W–65°W, 7°N–32°N) and the eastern side of the gyre (5°W–32°W, 7°N–40°N). Within these regions, the average δ^{15}N PON_{susp} was identified, and the percentage contribution of new N that N_2 fixation contributes to the PON_{susp} pool was then estimated using three boundary δ^{15}N values for deep nitrate (4‰, 4.5‰ and 5‰) and a value of −1‰ for N_2 fixation,

$$\left(\frac{\delta^{15}\mathrm{N\ PON_{susp}} - \delta^{15}\mathrm{N\ NO_3}}{\delta^{15}\mathrm{N\ N_2} - \delta^{15}\mathrm{N\ NO_3}}\right) \times 100\%. \quad (3)$$

[38] Given the three choices for the boundary values of deep NO_3^-, the percentage contribution of N from N_2 fixation to the PON_{susp} pool within the central part of the subtropical gyre is estimated to range between 72% (±5%)

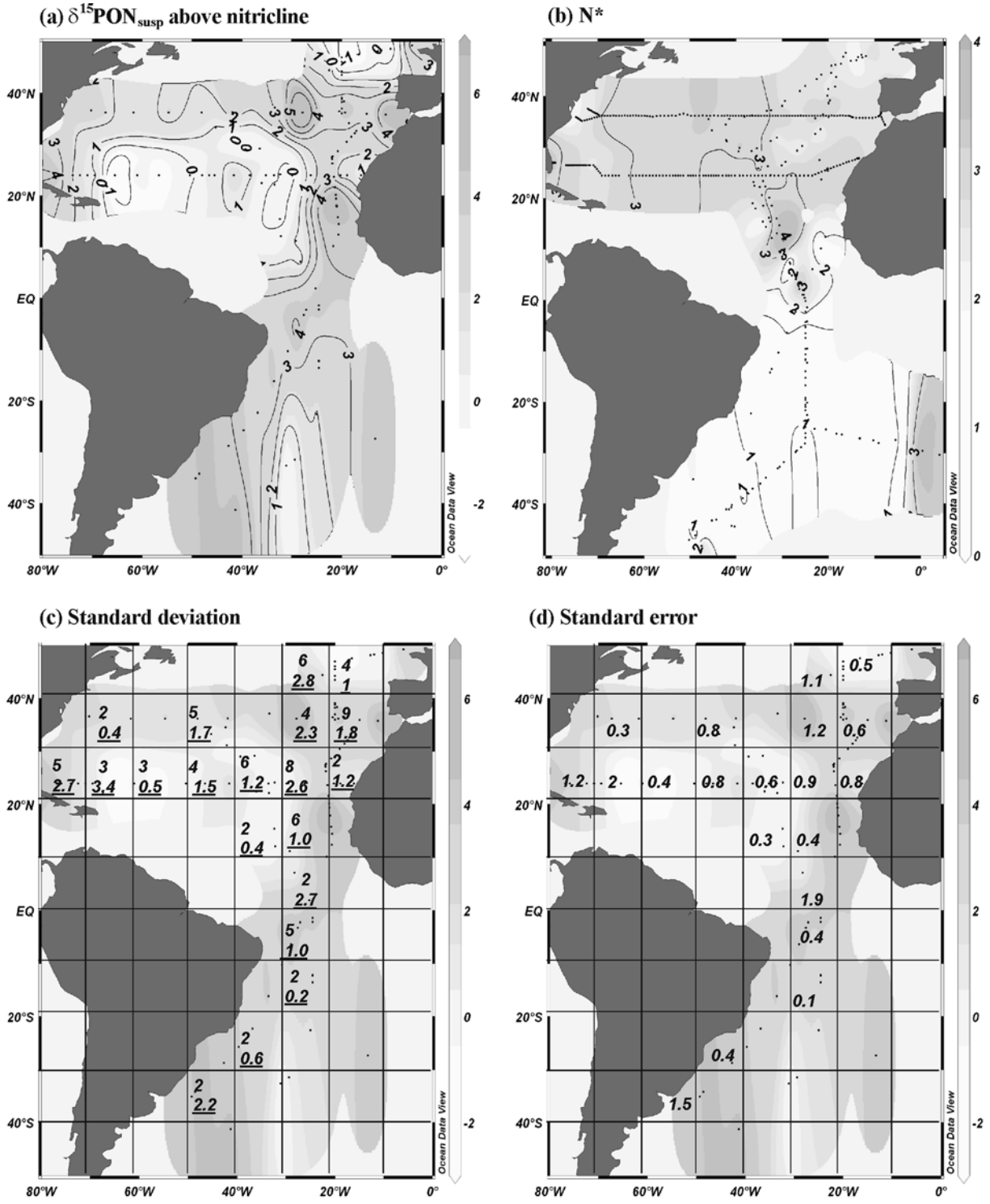

Figure 8. (a) Horizontal structure of δ^{15}N PON_{susp} above the nitricline demonstrating local patches of inferred N_2 fixation. (b) Widespread elevated N* values over entire northern basin, values averaged from below the nitricline to 300 m. (c) Standard deviation of δ^{15}N PON_{susp} (numbers underlined) along with the number of data points (above standard deviation). (d) Standard error of $\delta^{15}PON_{susp}$.

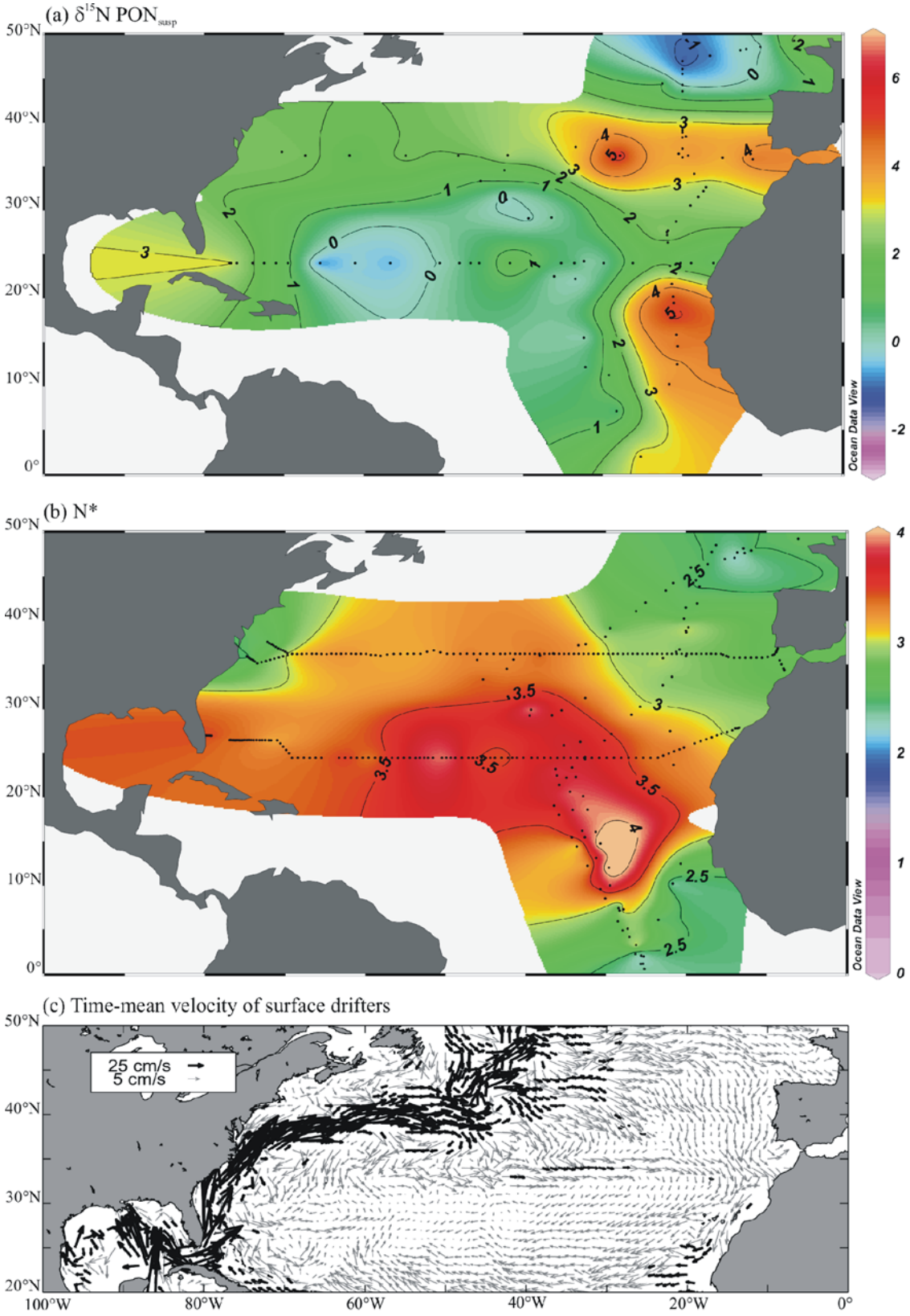
(a) δ15N PONsusp
50°N
40°N
30°N
20°N
10°N
0°
Ocean Data View
(b) N*
50°N
40°N
30°N
20°N
10°N
0°
Ocean Data View
(c) Time-mean velocity of surface drifters
25 cm/s
5 cm/s
50°N
40°N
30°N
20°N
100°W
80°W
60°W
40°W
20°W
0°

Figure 9

Table 2. Estimates of the Percentage Contribution of New N That N_2 Fixation Provides to the PON_{susp} Pool and Subsequently to the Total N Pool Over Separate Regions of the Northern Subtropical Gyre

	Northern Subtropical Gyre		
	Western Side (65°W–80°W, 20°N–40°N)	Center (30°W–65°W, 7°N–32°N)	Eastern Side (5°W–30°W, 7°N–40°N)
Average $\delta^{15}PON_{susp}$	**2.6**‰	**0.4**‰	**3.5**‰
n	7	22	29
Standard deviation	1.9	1.2	1.7
Standard error	0.7	0.3	0.3
Percent Contribution of N From N_2 Fixation to PON_{susp} ± Standard Error[a]			
4‰ for deep NO_3^- [b]	27% ± 15%	72% ± 5%	9% ± 7%
4.5‰ for deep NO_3^- [b]	34% ± 13%	74% ± 4%	18% ± 6%
5‰ for deep NO_3^- [b]	40% ± 12%	76% ± 4%	24% ± 6%
Nutrient Concentrations and Percent of Total N			
$[PON_{susp}]$,[c] % to total N pool	0.1 μM 1.9%	0.3 μM 6.8%	0.2 μM 4.7%
$[NO_3^-]$,[d] % to total N pool	0.1 μM 1.9%	0.02 μM 0.4%	0.08 μM 1.9%
[DON],[d] % to total N pool	5.1 μM 96.2%	4.1 μM 92.8%	4.0 μM 93.4%
Percent Contribution of N From N_2 Fixation Through PON_{susp} to Total N Pool ± Standard Error[a]			
4‰ for deep NO_3^- [b]	**0.5**% ± 0.3%	**4.9**% ± 0.3%	**0.4**% ± 0.3%
4.5‰ for deep NO_3^- [b]	**0.6**% ± 0.2%	**5.0**% ± 0.3%	**0.8**% ± 0.3%
5‰ for deep NO_3^- [b]	**0.8**% ± 0.2%	**5.1**% ± 0.3%	**1.3**% ± 0.3%

[a]Standard error associated with the $\delta^{15}N$ PON_{susp}, based upon ($\sigma/\sqrt{n}$), where σ is the standard deviation and n is the number of independent data points.
[b]*Knapp et al.* [2005], *Liu and Kaplan* [1989], and *Sigman et al.* [1997].
[c]Mean concentration (averaged above 1 μM nitricline) over region.
[d]Typical concentrations (averaged above 1 μM nitricline) for each region.

and 76% (±4%) (Table 2), with the errors representing the standard error of the $\delta^{15}PON_{susp}$ signals. On the western side of the gyre, the contribution of N_2 fixation was found to be lower in the range of 27% (±15%) to 40% (±12%) and lower again on the eastern side of the basin from 9% (±7%) to 24% (±6%). Hence, N_2 fixation is clearly important over the central part of the northern subtropical gyre in providing new N to the PON_{susp} pool, but less important on the western and eastern sides of the subtropical gyre. This difference suggests that other processes become important on the western and eastern sides of the gyre: On the western side, eddy transfer of nitrate close to the western boundary current is likely to be important [*Williams and Follows*, 2003] and, on the eastern side, the lateral transfer of nitrate and DON from coastal upwelling [*Roussenov et al.*, 2006].

5.2. Role of N_2 Fixation in Providing New N to the Total N Pool

[39] The isotopic calculation is now extended to estimate the percentage contribution of new N that N_2 fixation introduces via PON_{susp} to the total N pool. The total N pool is defined here by DON, NO_3^- and PON_{susp}; while PON_{sink} is important in the export of N out of the euphotic zone, PON_{sink} makes only a minor contribution to the total N pool [*Wakeham and Lee*, 1989]. Within the centre of the northern gyre, the PON_{susp} pool represents only ~6.8% of the total N (Figure 1a and Table 2). Thus the average contribution of new N supplied from N_2 fixation via PON_{susp} to the total N pool is 5.0% (±0.3%) again with the errors representing the standard error of the $\delta^{15}PON_{susp}$ signals for the region (Table 2, assuming 4.5‰ for the deep nitrate). At the western and eastern sides of the gyre the contribution of new N supplied from N_2 fixation via the PON_{susp} are even smaller and only typically reach 0.6% (±0.2%) and 0.8% (±0.3), respectively.

[40] The contributions of NO_3^- and DON now need to be considered in the total N pool. DON dominates the total N pool in surface waters accounting for 93–96% across the northern basin, while surface NO_3^- represents only 0.4–1.9% of the total N pool. While no measurements of $\delta^{15}N$ NO_3^- or $\delta^{15}N$ DON were made in the present study, data are available from BATS with typical values of 3.5‰ for surface NO_3^- and 4‰ for DON (Table 3) [*Knapp et al.*, 2005]. Using these data, applying the two-end-member mixing model (3) to the western side of the northern subtropical gyre suggests that the new N supplied to the total N pool from N_2 fixation via DON is 8.2% (±8%) and via NO_3^- is 0.3% (±0.1%) with the error range now representing the standard deviation of the estimates obtained from the choice of three boundary $\delta^{15}N$ values for deep NO_3^-. Thus our estimate of the total supply of new N from N_2 fixation reaches 9.2% (±4.5%) over the western side of the northern subtropical gyre. If the same calculations were applied to the central and eastern regions of the North Atlantic including the DON and NO_3^- pools there (Table 2), the total supply of new N from N_2 fixation would

Figure 9. (a) The $\delta^{15}N$ PON_{susp} above the nitricline for the North Atlantic, depleted signal seen over much of the central subtropical gyre; (b) N* (values averaged below the nitricline down to 300 m) for the North Atlantic; and (c) time-mean velocity of surface drifters [*Lumpkin and Pazos*, 2006]. Westward flow of 5 cm s^{-1} at 20°N coincides with elevated N*, revealing the nonconservative behavior of N*. Probable region of N_2 fixation in the North Atlantic is between 30°W–50°W and 15°N–30°N.

Table 3. Two-End-Member Mixing Model (4) Applied to Surface NO_3^- and DON to Gain an Estimate for the Percentage Contribution of New N That N_2 Fixation Makes Via Surface PON_{susp}, NO_3^-, and DON Over the Western Side of the Northern Subtropical Gyre

	Western Side (65°W–80°W, 20°N–40°N)			
Northern Subtropical Gyre	4 ‰ for Deep NO_3^-	4.5‰ for Deep NO_3^-	5‰ for Deep NO_3^-	Mean ± Standard Deviation[a]
[PON_{susp}] and % to total N pool[b]	0.1 μM 1.9%	0.1 μM 1.9%	0.1 μM 1.9%	
Percent contribution of N from N_2 fixation through PON_{susp} to total N pool	0.5%	0.7%	0.8%	**0.6%** ± 0.1
[NO_3^-] and % to total N pool[c]	0.1 μM 1.9%	0.1 μM 1.9%	0.1 μM 1.9%	
Percent contribution from N_2 fixation through surface NO_3^- to total N pool	0.2%	0.3%	0.5%	**0.3%** ± 0.1
[DON] and % to total N pool[c]	5.1 μM 96.2%	5.1 μM 96.2%	5.1 μM 96.2%	
Percent contribution from N_2 fixation through DON to total N pool	0%	8.7%	16.1%	**8.2%** ± 8.0
Total % contribution from N_2 fixation to total N pool				**9.2%** ± 4.5

[a]Standard deviation of the estimates obtained from the three boundary values chosen for deep NO_3^-.
[b]Details in Table 2.
[c]Typical concentrations (averaged above 1 μM nitricline) for region. Range of boundary values used for deep NO_3^- while δ^{15}DON is 4‰, and δ^{15}N surface NO_3^- is 3.5‰ (average at 100 m at BATS) [*Knapp et al.*, 2005].

be 13.7% and 9.2%, respectively. However, since it is unlikely that δ^{15}N DON or δ^{15}N NO_3^- are the same across the entire northern basin, these estimates are speculative. Further work is necessary to determine the stable N isotopic composition of components of the N pool in order to understand the different sources of N utilized by phytoplankton.

5.3. Wider Context

[41] The isotopic mass balance method employed in this study reveals that nitrogen fixation varies over the northern subtropical gyre, accounting for 72% to 76% of the PON_{susp} in the central region (30°W–65°W, 7°N–32°N) and 27% to 40% in the western region of the gyre (65°W–80°W, 20°N–40°N). In comparison, using the same method, *Montoya et al.* [2002] estimates the contribution of nitration fixation to PON_{susp} of 30–40% over the tropics (25°W–60°W, 0°–15°N) and the western side of the gyre (42°W–80°W, 7°N–28°N); likewise, *Capone et al.* [2005] estimates a similar contribution of 36% over the western side of the gyre (42°W–80°W, 7°N–28°N). These estimates of *Montoya et al.* [2002] and *Capone et al.* [2005] are consistent with our estimates over our western region, but are lower than our estimates over the central region of the subtropical gyre. *Montoya et al.* [2002] and *Capone et al.* [2005] used the same two-end-member mixing model (3), but with a more depleted δ^{15}N value for N_2 fixation of −2‰, rather than our boundary value of −1‰. Our estimates for nitrogen fixation for the central region only decrease to 60–65% when this lower boundary value of −2‰ is instead used. Thus the contrasting estimates of nitrogen fixation over the central part of the subtropical gyre reflect differences in the isotopic data for PON_{susp}.

[42] On previous AMT cruises (1–8), the nitrogen-fixing cyanobacteria *Trichodesmium* spp. was found to be most abundant to the north of the equator (0°–15°N). *Tyrrell et al.* [2003] estimated the nitrogen fixation provided >20% of total new N input in these tropical waters. This estimate is greater than our estimates of nitrogen fixation providing ~9% of the total N pool in the western North Atlantic and the speculative 14% in the central part of the subtropical gyre, but these difference might easily be accounted for by the different regions, timing and uncertainties in the studies.

[43] In our view, N_2 fixation leads to the extensive depleted δ^{15}N PON_{susp} over the North Atlantic subtropical gyre, as well as the westward increase in N* following the gyre circulation along 20°N. This view is in accord with independent studies suggesting that N_2 fixation occurs in the Atlantic Ocean and provides a significant source of N phytoplankton to the subtropical Northern gyre [*Capone et al.*, 2005; *Gruber and Sarmiento*, 1997; *Michaels et al.*, 1996]. However, the importance of N_2 fixation in providing an area-integrated flux is uncertain, since estimates range from 0.03–0.3 mol N m^{-2} a^{-1} (see *Capone et al.* [2005] for full details). This uncertainty reflects the difficulty of providing area-averaged estimates for a process associated with blooms, which are spatially heterogeneous and often short-lived.

6. Conclusions

[44] A unique data set of stable isotopic data for δ^{15}N PON_{susp} is presented for the Atlantic Ocean. Over the central part of the subtropical northern gyre, there was an extensive signal of depleted δ^{15}N PON_{susp}. This signal was persistent and robust, being observed over 3 years both in Northern Hemisphere spring and autumn. The PON_{susp} signal was primarily autotrophic rather than heterotrophic, based upon interpretation of the isotopic signals, particulate organic carbon, nitrogen and chlorophyll *a* levels.

[45] The extensive depleted isotopic signal might be formed either by N_2 fixation or recycling. N_2 fixation appears to be the more plausible explanation, since the depleted signals occur in a region where there is a westward increase in the quasi-conservative tracer N* following the gyre circulation along 20°N.

[46] Estimates of the percentage contribution of new N that N_2 fixation introduces via the PON_{susp} pool to the total N pool have been calculated using a two-end-member mixing model. This estimate typically reaches ~74% in the centre of the oligotrophic gyre. Since the phytoplankton are included in the PON_{susp} pool, this underlines the importance of N_2 fixation as a source of new N to the primary producers. However, PON_{susp} accounts for only ~6.8% of total N in the center of the gyre, so the contribution to the total N pool of new N from N_2 fixation is only 5%. If this estimate is repeated at the western side of the gyre including isotopic values for NO_3^- and DON [*Knapp et al.*, 2005], then ~9% of new N can be accounted for by N_2 fixation. This estimate is likely to be only slightly higher over the central part of the subtropical gyre, but further isotopic values are needed for DON and surface NO_3^- to provide a reliable estimate. It seems, therefore, that N_2 fixation can be an important source of N to the phytoplankton, but is unlikely to account for the mismatch in the supply of N and the observed export production for the subtropical gyre. There is clearly a need for further work in obtaining measurements of $\delta^{15}N$ NO_3^- and DON in the North Atlantic in order to identify the relative importance of the different pathways of N through the marine system.

[47] **Acknowledgments.** This study was supported by the UK Natural Environment Research Council through the Atlantic Meridional Transect consortium (NER/O/S/2001/00680) and the 36°N consortium (NER/O/S/2003/00625). We would like to thank Katie Chamberlain, Sinhue Torres, and Tim Lesworth for their assistance in the analysis of nutrients, Alex Poulton for the analysis of chlorophyll. *a*, the officers, crew and UKORS staff of RRS *James Clark Ross*, RRS *Discovery*, and RRS *Charles Darwin*. Thanks go also to Robert Petty at the Marine Science Institute Analytical Lab, University of California, for isotopic analysis. This is contribution 150 of the AMT Programme.

References

Altabet, M. A. (1988), Variations in nitrogen isotopic composition between sinking and suspended particles: Implications for nitrogen cycling and particle transformation in the open ocean, *Deep Sea Res.*, *35*, 535–554.

Altabet, M. A. (1996), Nitrogen and carbon isotopic tracers of the source and transformation of particles in the deep sea, in *Particle Flux in the Ocean*, edited by V. Ittekkot et al., pp. 155–184, John Wiley, Hoboken, N. J.

Altabet, M. A., and J. J. McCarthy (1985), Temporal and spatial variations in the natural abundance of ^{15}N in PON from a warm-core ring, *Deep Sea Res., Part A*, *32*, 755–772.

Altabet, M. A., W. G. Deuser, S. Honjo, and C. Stienen (1991), Seasonal And Depth–Related Changes In The Source Of Sinking Particles In The North-Atlantic, *Nature*, *354*, 136–139.

Baker, A. R., S. D. Kelly, K. F. Biswas, M. Witt, and T. D. Jickells (2003), Atmospheric deposition of nutrients to the Atlantic Ocean, *Geophys. Res. Lett.*, *30*(24), 2296, doi:10.1029/2003GL018518.

Berman, T., and D. A. Bronk (2003), Dissolved organic nitrogen: A dynamic participant in aquatic ecosystems, *Aquat. Microb. Ecol.*, *31*, 279–305.

Biggs, D. C. (1977), Respiration and ammonium excretion by open ocean gelatinous zooplankton, *Limnol. Oceanogr.*, *22*, 108–117.

Capone, D. G., J. P. Zehr, H. W. Paerl, B. Bergman, and E. J. Carpenter (1997), *Trichodesmium*, a globally significant marine cyanobacterium, *Science*, *276*, 1221–1229.

Capone, D. G., J. A. Burns, J. P. Montoya, A. Subramaniam, C. Mahaffey, T. Gunderson, A. F. Michaels, and E. J. Capenter (2005), Nitrogen fixation by *Trichodesmium* spp.: An important source of new nitrogen to the tropical and subtropical North Atlantic Ocean, *Global Biogeochem. Cycles*, *19*, GB2024, doi:10.1029/2004GB002331.

Carpenter, E. J., H. R. Harvey, B. Fry, and D. G. Capone (1997), Biogeochemical tracers of the marine cyanobacterium *Trichodesmium*, *Deep Sea Res., Part I*, *44*, 27–38.

Charette, M. A., S. Bradley Moran, and J. K. B. Bishop (1999), ^{234}Th as a tracer of particulate organic carbon export in the subarctic northeast Pacific Ocean, *Deep Sea Res., Part II*, *46*, 2833–2861.

Checkley, D. M., and C. A. Miller (1989), Nitrogen isotopic fractionation by oceanic zooplankton, *Deep Sea Res.*, *36*, 1449–1456.

Corner, E. D. S., and A. G. Davies (1971), Plankton as a factor in the nitrogen and phosphorus cycles in sea, *Adv. Mar. Biol.*, *9*, 101–204.

Dentener, F., et al. (2006), Nitrogen and sulfur deposition on regional and global scales: A multimodel evaluation, *Global Biogeochem. Cycles*, *20*, GB4003, doi:10.1029/2005GB002672.

Deutsch, C., N. Gruber, R. M. Key, J. L. Sarmiento, and A. Ganachaud (2001), Denitrification and N-2 fixation in the Pacific Ocean, *Global Biogeochem. Cycles*, *15*, 483–506.

Emerson, S., P. Quay, D. Karl, C. Winn, L. Tupas, and M. Landry (1997), Experimental determination of the organic carbon flux from open ocean surface waters, *Nature*, *389*, 951–954.

Fogel, M. L., and L. A. Cifuentes (1993), Isotope fractionation during primary production, in *Organic Geochemistry—Principles and Applications*, edited by M. H. Engel and S. A. Macko, pp. 73–98, Plenum, New York.

Galloway, J. N., et al. (2004), Nitrogen cycles: Past, present, and future, *Biogeochemistry*, *70*, 153–226.

Gruber, N., and J. L. Sarmiento (1997), Global patterns of nitrogen fixation and denitrification, *Global Biogeochem. Cycles*, *11*, 235–266.

Hansell, D. A., N. R. Bates, and D. B. Olson (2004), Excess nitrate and nitrogen fixation in the North Atlantic Ocean, *Mar. Chem.*, *84*, 243–265.

Hastings, M. G., D. M. Sigman, and F. Lipschultz (2003), Isotopic evidence for source changes of nitrate in rain at Bermuda, *J. Geophys. Res.*, *108*(D24), 4790, doi:10.1029/2003JD003789.

Jackson, G. A., and P. M. Williams (1985), Importance of dissolved organic nitrogen and phosphorus to biological nutrient cycling, *Deep Sea Res.*, *32*, 223–235.

Jenkins, W. J., and C. Goldman (1985), Seasonal oxygen cycling and primary production in the Sargasso Sea, *J. Mar. Res.*, *43*, 465–491.

Karl, D., A. Michaels, B. Bergman, D. Capone, E. Carpenter, R. Letelier, F. Lipschultz, H. Paerl, D. Sigman, and L. Stal (2002), Dinitrogen fixation in the world's oceans, *Biogeochemistry*, *57/58*, 47–98.

Kiriakoulakis, K., B. J. Bett, M. White, and G. A. Wolff (2004), Organic biogeochemistry of the Darwin Mounds, a deep-water coral ecosystem, of the NE Atlantic, *Deep Sea Res., Part I*, *51*, 1937–1954.

Knapp, A. N., D. M. Sigman, and F. Lipschultz (2005), N isotopic composition of dissolved organic nitrogen and nitrate and the Bermuda Atlantic Time-series Study site, *Global Biogeochem. Cycles*, *19*, GB1018, doi:10.1029/2004GB002320.

Landolfi, A. (2005), The importance of dissolved organic nutrients in the biogeochemistry of oligotrophic gyres, Ph.D. thesis, Natl. Oceanogr. Cent., Southampton, U. K.

Levy, M., P. Klein, and A. Treguier (2001), Impact of sub-mesoscale physics on production and subduction of phytoplankton in the oligotrophic regime, *J. Mar. Res.*, *59*, 535–565.

Liu, K.-K., and I. R. Kaplan (1989), The eastern tropical Pacific as a source of ^{15}N-enriched nitrate in seawater off southern California, *Limnol. Oceanogr.*, *34*, 820–830.

Lumpkin, R., and M. Pazos (2006), Measuring surface currents with Surface Velocity Program drifters: The instrument, its data, and some recent results, in *Lagrangian Analysis and Prediction of Coastal and Ocean Dynamics (LAPCOD)*, edited by A. Griffa et al. chap. 2, pp. 39–67, Cambridge Univ. Press, Cambridge, U. K.

Mahaffey, C., R. G. Williams, G. A. Wolff, N. Mahowald, W. Anderson, and M. Woodward (2003), Biogeochemical signatures of nitrogen fixation in the eastern North Atlantic, *Geophys. Res. Lett.*, *30*(6), 1300, doi:10.1029/2002GL016542.

Mahaffey, C., R. G. Williams, and G. A. Wolff (2004), Physical supply of nitrogen to phytoplankton in the Atlantic Ocean, *Global Biogeochem. Cycles*, *18*, GB1034, doi:10.1029/2003GB002129.

Mahaffey, C., A. F. Michaels, and D. G. Capone (2005), The conundrum of marine N-2 fixation, *Am. J. Sci.*, *305*, 546–595.

McGillicuddy, D. J., A. R. Robinson, D. A. Siegel, H. W. Jannasch, R. Johnson, T. D. Dickey, J. McNeil, A. F. Michaels, and A. H. Knap (1998), Influence of mesoscale eddies on new production in the Sargasso Sea, *Nature*, *394*, 263–265.

Michaels, A. F., N. R. Bates, K. O. Buessler, C. A. Carlson, and A. H. Knap (1994), Carbon-cycle imbalances in the Sargasso Sea, *Nature*, *372*, 537–540.

Michaels, A. F., D. Olson, J. L. Sarmiento, J. W. Ammerman, K. Fanning, R. Jahnke, A. H. Knap, F. Lipschultz, and J. M. Prospero (1996), Inputs, losses and transformations of nitrogen and phosphorus in the pelagic north Atlantic ocean, *Biogeochemistry*, *25*, 181–226.

Mills, M. M., C. Ridame, M. Davey, J. L. Roche, and R. J. Geider (2004), Iron and phosphorus co-limit nitrogen fixation in the eastern tropical North Atlantic, *Nature*, *429*, 292–432.

Minagawa, M., and E. Wada (1986), Nitrogen isotope ratios of red tide organisms in the East China Sea: A characterisation of biological nitrogen fixation, *Mar. Chem.*, *19*, 245–259.

Montoya, J. P., and J. J. McCarthy (1995), Isotopic fractionation during nitrate uptake by phytoplankton grown in continuous culture, *J. Plankton Res.*, *17*, 439–464.

Montoya, J. P., et al. (2002), Nitrogen fixation and nitrogen isotope abundances in zooplankton of the oligotrophic North Atlantic, *Limnol. Oceanogr.*, *47*, 1617–1628.

Montoya, J. P., C. M. Holl, J. P. Zehr, A. Hensen, T. A. Villareal, and D. G. Capone (2004), High rates of N_2 fixation by unicellular diatrophs in the oligotrophic Pacific Ocean, *Nature*, *430*, 1027–1031.

Nakatsuka, T., N. Handa, N. Harada, T. Sugimoto, and S. Imaizumi (1997), Origin and decomposition of sinking particulate organic matter in the deep water column inferred form the vertical distributions of its $\delta^{15}N$, $\delta^{13}C$ and $\delta^{14}C$, *Deep Sea Res., Part I*, *44*, 1957–1979.

Orcutt, K. M., F. Lipschultz, K. Gundersen, R. Arimoto, A. F. Micheals, A. H. Knap, and J. R. Gallon (2001), A seasonal study of the significance of N_2 fixation by *Trichodesmium* spp. at the Bermuda Atlantic Time-series Study (BATS) site, *Deep Sea Res., Part II*, *48*, 1583–1608.

Owens, N. J. P. (1987), Natural variations in ^{15}N in the marine environment, *Adv. Mar. Biol.*, *24*, 389–451.

Polovina, J. J., G. T. Mitchum, and G. T. Evans (1995), Decadal and basin-scale variation in mixed layer depth and the impact on biological production in the Central and North Pacific, 1960–88, *Deep Sea Res., Part I*, *42*, 1701–1716.

Prospero, J. M., K. Barrett, T. Church, F. Dentener, R. A. Duce, J. N. Galloway, H. Levy, J. Moody, and P. Quinn (1996), Atmospheric deposition of nutrients to the North Atlantic Basin, *Biogeochemistry*, *35*, 27–73.

Redfield, A. C. (1958), The biological control of chemical factors in the environment, *Am. Sci.*, *46*, 205–221.

Robinson, C., A. J. Poulton, P. M. Holligan, A. R. Baker, G. Forster, N. Gist, T. D. Jickells, G. Malin, R. Upstill-Goddard, and R. G. Williams (2006), The Atlantic Meridional Transect (AMT) Programme: A contextual view 1995–2005, *Deep Sea Res., Part II*, *53*, 1485–1515.

Roussenov, V., R. G. Williams, C. Mahaffey, and G. A. Wolff (2006), Does the transport of dissolved organic nutrients affect export production in the Atlantic Ocean?, *Global Biogeochem. Cycles*, *20*, GB3002, doi:10.1029/2005GB002510.

Sanders, R., and T. Jickells (2000), Total organic nutrients in Drake Passage, *Deep Sea Res., Part I*, *47*, 997–1014.

Sigman, D. M., M. A. Altabet, R. Michener, D. C. McCorkle, B. Fry, and R. M. Holmes (1997), Natural abundance-level measurement of the nitrogen isotopic composition of oceanic nitrate: An adaptation of the ammonia diffusion method, *Mar. Chem.*, *57*, 227–242.

Tyrrell, T., E. Maranon, A. J. Poulton, A. R. Bowie, D. S. Harbour, and E. M. S. Woodward (2003), Large-scale latitudinal distribution of Trichodesmium spp. in the Atlantic Ocean, *J. Plankton Res.*, *25*, 405–416.

Voss, M., M. A. Altabet, and B. von Bodungen (1996), $\delta^{15}N$ in sedimenting particles as indicator of euphotic zone processes, *Deep Sea Res., Part I*, *43*, 33–46.

Wakeham, S. G., and C. Lee (1989), Organic geochemistry of particulate matter in the ocean: The role of particles in oceanic sedimentary cycles, *Org. Geochem.*, *14*, 83–96.

Waser, N. A. D., W. G. Harrison, E. J. H. Head, B. Nielsen, V. A. Lutz, and S. A. Calvert (2000), Geographic variations in the nitrogen isotope composition of surface particulate nitrogen and new production across the North Atlantic Ocean, *Deep Sea Res., Part I*, *47*, 1207–1226.

Welschmeyer, N. A. (1994), Fluorometric analysis of chlorophyll-a in the presence of chlorophyll-*b* and pheopigments, *Limnol. Oceanogr.*, *39*, 1985–1992.

Williams, R. G., and M. J. Follows (2003), Physical transport of nutrients and the maintenance of biological production, in *Ocean Biogeochemistry: The Role of the Ocean Carbon Cycle in Global Change*, edited by M. Fasham, pp. 19–51, Springer, New York.

Woodward, E. M. S., and A. P. Rees (2001), Nutrient Distributions in an anticyclonic gyre in the northeast Atlantic Ocean, with reference to nanomolar ammonium concentrations, *Deep Sea Res., Part II*, *48*, 775–793.

Yamamuro, M., and H. Kayanne (1995), Rapid direct determination of organic-carbon and nitrogen in carbonate-bearing sediments with a Yanaco Mt-5 Chn Analyzer, *Limnol. Oceanogr.*, *40*, 1001–1005.

A. Landolfi, Biogeochemical Modeling, Leibniz Institute of Marine Sciences, Dienstgebäude Westufer, Düsternbrooker Weg 20, D-24105 Kiel, Germany.

R. L. Mather, R. G. Williams, and G. A. Wolff, Department of Earth and Ocean Sciences, University of Liverpool, 4 Brownlow Street, Liverpool L69 3GP, UK.

S. E. Reynolds, Department of Ocean, Earth and Atmospheric Sciences, Old Dominion University, 4600 Elkhorn Avenue, Norfolk, VA 23529-0276, USA. (sereynolds@odu.edu)

R. Sanders, National Oceanography Centre, University of Southampton Waterfront Campus, European Way, Southampton SO14 3ZH, UK.

E. M. S. Woodward, Plymouth Marine Laboratory, Prospect Place, The Hoe, Plymouth PL1 3DH, UK.